Electronic Supplementary Material (ESI) for Soft Matter.

Supporting Information:

Fibrin formation and fractal organization at cationic, anionic, and zwitterionic polymer coated interfaces

Achebe N.O. Nzulumike[1,2], Robert A. Biro[1], Esben Thormann[1*]

[1]Department of Chemistry, Technical University of Denmark, 2800 Kgs. Lyngby, Denmark

[2]Department of Mechanical Engineering, Technical University of Denmark, 2800 Kgs. Lyngby, Denmark

*esth@kemi.dtu.dk

S1. Topography of Charged Polymer Surfaces

Charged polymer coatings were topographically characterized by atomic force microscopy (AFM) and representative images are presented in Fig. S1. All coatings featured very uniform topography, as evidenced by consistently narrow height distributions (less than a 3 nm range), and exhibited high smoothness, as the root mean square (RMS) roughness was determined to consistently be less than 0.6 nm. This high uniformity and smoothness confirms the applicability of these coatings as substrates for surface-dependent fibrin formation.

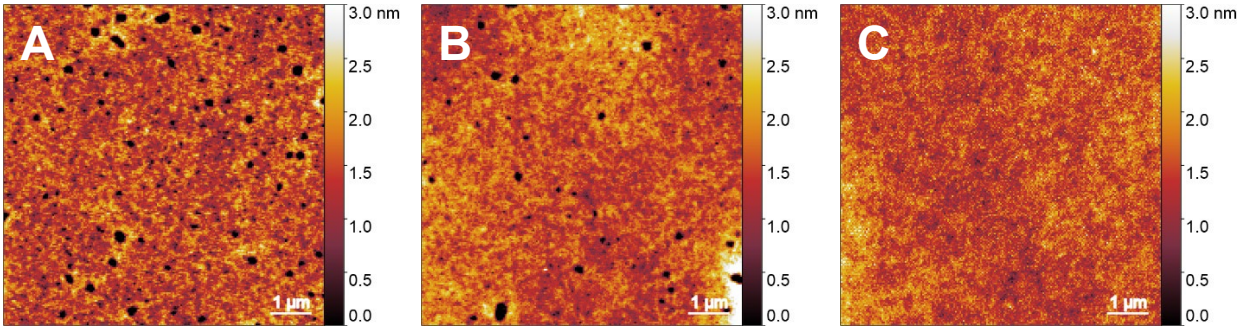

Figure S1. Topography of charged polymer surfaces. Cationic (A), anionic (B), and zwitterionic (C) coatings, all of which feature RMS roughness < 6 Å.

S2. Sample Drying and Control Experiments

Fibrin was formed by mixing clotting factor proteins under flow, followed by extracting the clotted samples from the flow system and immediately removing liquid by using capillary action. This was achieved by carefully holding porous filter paper to the edge of the freshly exposed substrate. Generally, the resulting structures on charged surfaces included a distribution of fractal morphologies, as seen in Fig. 2 and 4. However, as the exchange of medium from liquid to air may affect the resulting structures, a number of control experiments were conducted to assess the potential impact on clot morphology.

A set of experiments were conducted without proteins, exposing the substrate to pure saline solution without fibrinogen or thrombin (Fig. S2 top). The resulting samples were essentially featureless, indicating the complete removal of saline and thus precluding significant depositions of salt crystals on the surface.

A set of experiments were conducted without thrombin, which is associated with enzymatic conversion of fibrinogen into fibrin monomers (Fig. S2 middle). The resulting samples were predominantly unclotted, yielding no distinct structures with either fractal or fibrous morphology. The limited adsorbates are attributed to unpolymerized fibrinogen aggregates, as expected based on QCM frequency evolution in Fig. 2A.

A set of experiments were conducted without flow, and instead had the substrates incubated in freshly mixed clotting factors (Fig. S2 bottom). This static fibrin formation resulted in well-defined fibrous structures, which is the expected native structure for fibrin both *in vitro* and *in vivo*.[4–6] The fibers had an approximate thickness (diameter) of 50 nm, a length scale comparable to that of the fractal branches seen in Fig. 2C.

Thus, we have shown that all the tested aspects are necessary prerequisites to form fractal branched fibrin structures. Notably, fractal morphologies do not appear to be caused alone by the capillarity-based drying procedure or salt crystallization. Further experiments have shown that fractal morphologies can also form on chemically varied polymeric substrates (data not shown).

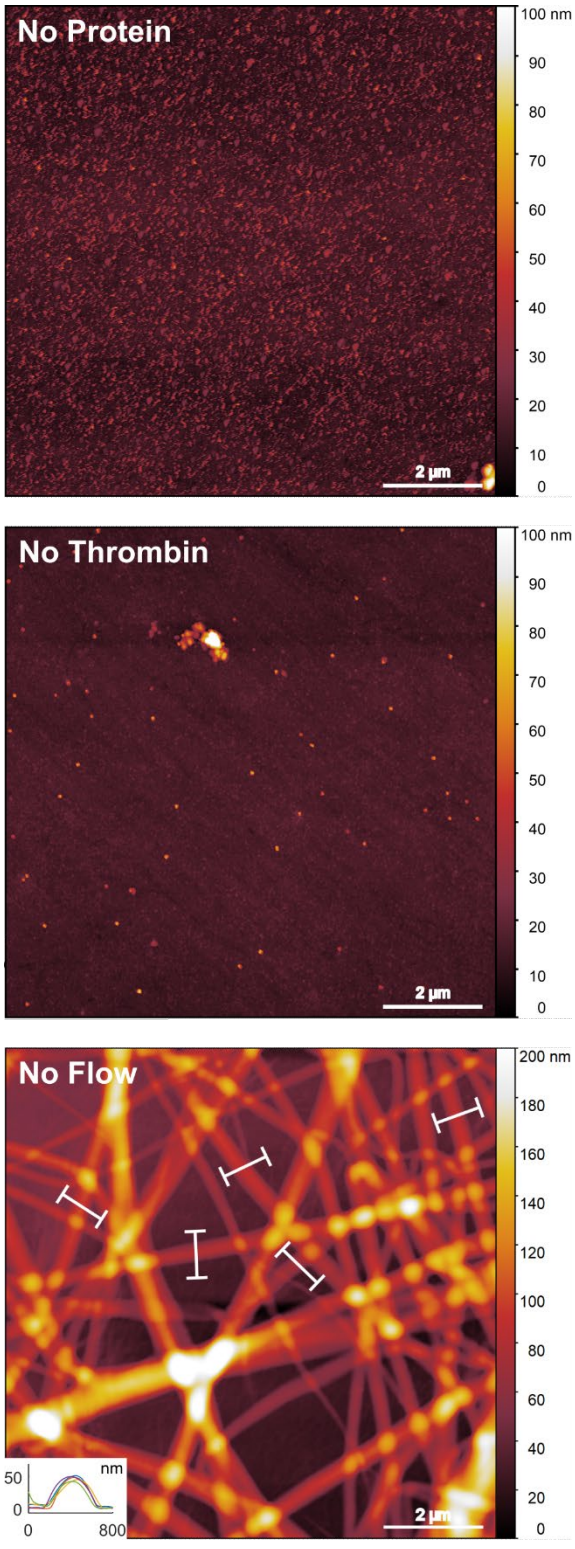

Figure S2. Control experiments related to morphology. Omission of proteins (top) or only thrombin (middle) yield no distinct features, whereas omission of flow (bottom) yields fiber morphologies with approximate diameters measured by line profiles (inset).

S3. Fractal Analysis

Fractal analysis characterizes pattern complexity, i.e. how the number of discrete spatial features changes with the scale of observation.[1] This complexity is quantified as one or more fractal dimensions,[2] in context of the following scaling relationship:

$$N \propto \varepsilon^{-D_F}$$

Here N is the number of observable features (e.g. discrete geometric objects), ε is the scaling factor (magnification factor), and D_F is the fractal dimension.

We analyzed fractal branched morphologies in AFM images using the FracLac plugin for ImageJ software, which determines fractal dimensions by box counting[3] (Fig. S3). Box counting is a sampling process where a grid is layered over a binary image, followed by counting the number of grid-boxes N that contain featured pixels (those with a binary positive value). By repeating this process for grids of progressively smaller box sizes, we get the relative scaling, ε, whereby we can derive the fractal dimension as the slope of $\ln N$ vs $\ln \varepsilon$.

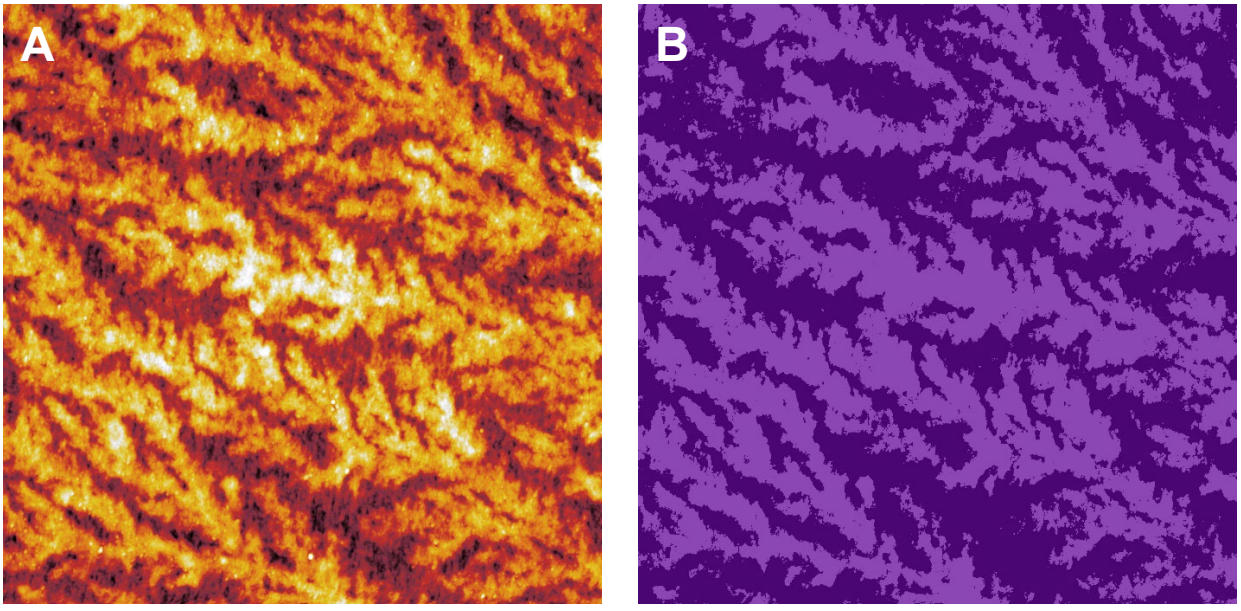

Figure S3. Fractal analysis of fibrin on silica surfaces, scanned by AFM in 10x10 μm^2 area. A: Pre-processed image, color range 0-100 nm. B: Binary 8-bit image version for fractal analysis, with the features of interest marked by bright pixels. Fractal dimension was here 1.79 ± 0.04.

S4. Fibrin Adsorption at varying Flow Rate

Fibrin adsorption is primarily quantified as the mass increase after loading mixed clotting factors. While retaining the same volume exchange at each step of fibrin formation, a decrease in flow rate from 0.100 mL/min to 0.050 mL/min (a factor 2) yields an increase in adsorption from 17.6 to 82.9 mg/m^2 (a factor 4.7), suggesting an inverse scaling relationship (Fig. S4). As half flow rate effectively results in double mixing time, this quintuple increase in mass shift is attributed to the clotting factors combining and forming fibrin over twice the duration.

Conversely, the initial fibrinogen adsorption is unaffected by concentration or flow rate, with consistent adsorption values of 8.6-12 mg/m^2. This confirms that the surface has been thoroughly saturated, as neither fibrinogen volume density nor flow rate would change the number of available fibrinogen binding sites. The final adsorbed mass is similarly independent of concentration and rate, with Δm_a ending at a total 21-23 mg/m^2. A consistent fraction of protein mass is thus retained after rinsing, suggesting that most of the fibrin is weakly attached to the surface.

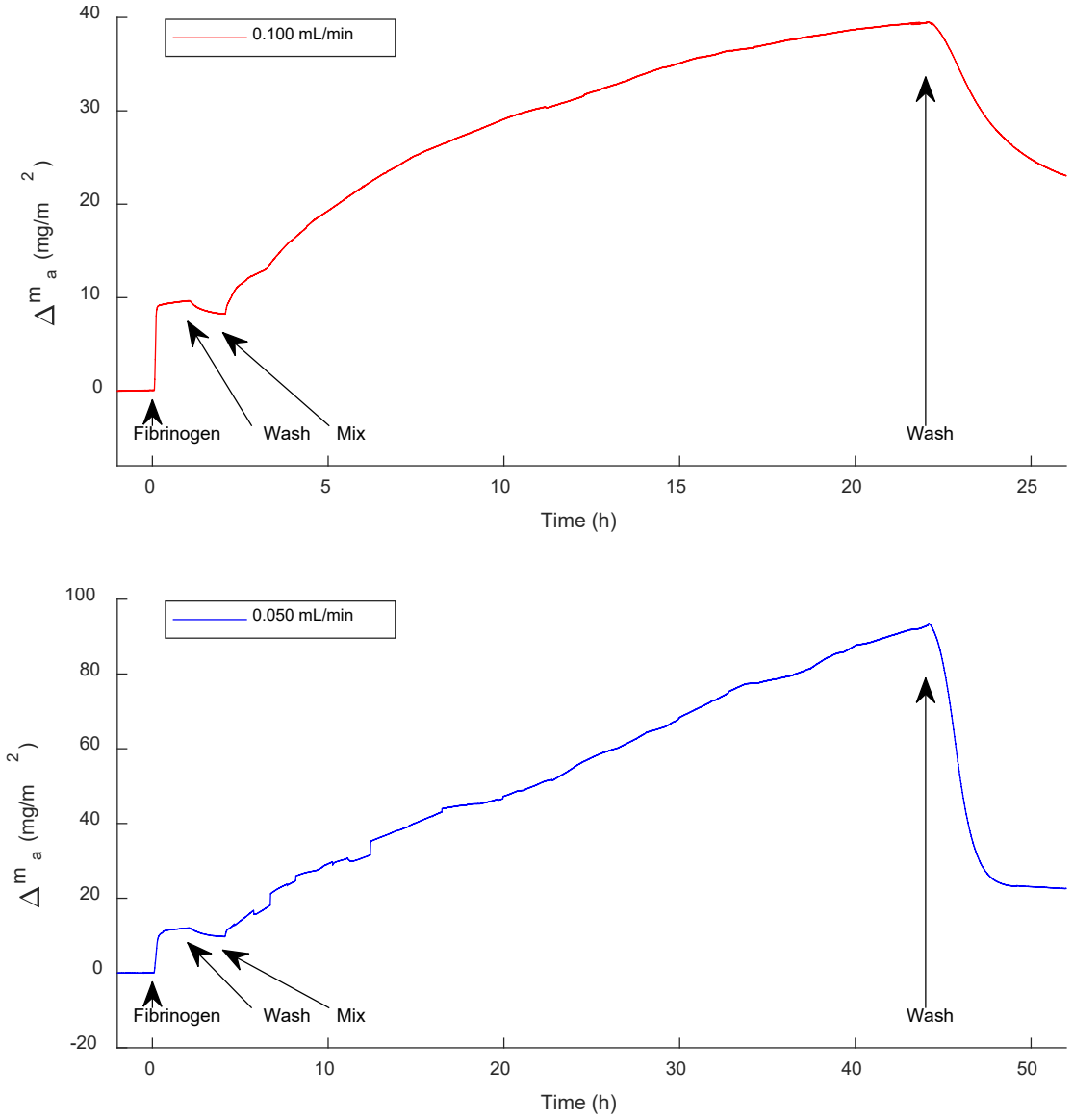

Figure S4. Fibrin adsorbed mass scales with flow rate. Fibrin formation at 0.100 (A) and 0.050 (B) mL/min. Note that the same volume is loaded during each sample step, necessitating a factor 2 difference in time intervals between the two measurements.

S5. Optical Imaging

Optical imaging of clotted charged polymer coatings reveal spatial distributions of fibrin morphologies (Fig. S5). These structures are highly heterogeneous, but can generally be categorized as either fractal branches or amorphous aggregates. By acquiring images over large areas (minimal objective magnification), some general trends emerge for surface-dependent fibrin organization. Cationic surfaces featured the highest relative coverage of amorphous aggregates, and anionic surfaces featured the highest relative coverage of fractal branches. Zwitterionic surfaces had the overall lowest coverage, with a fractal-to-aggregate distribution intermediate between that of cationic and anionic surfaces.

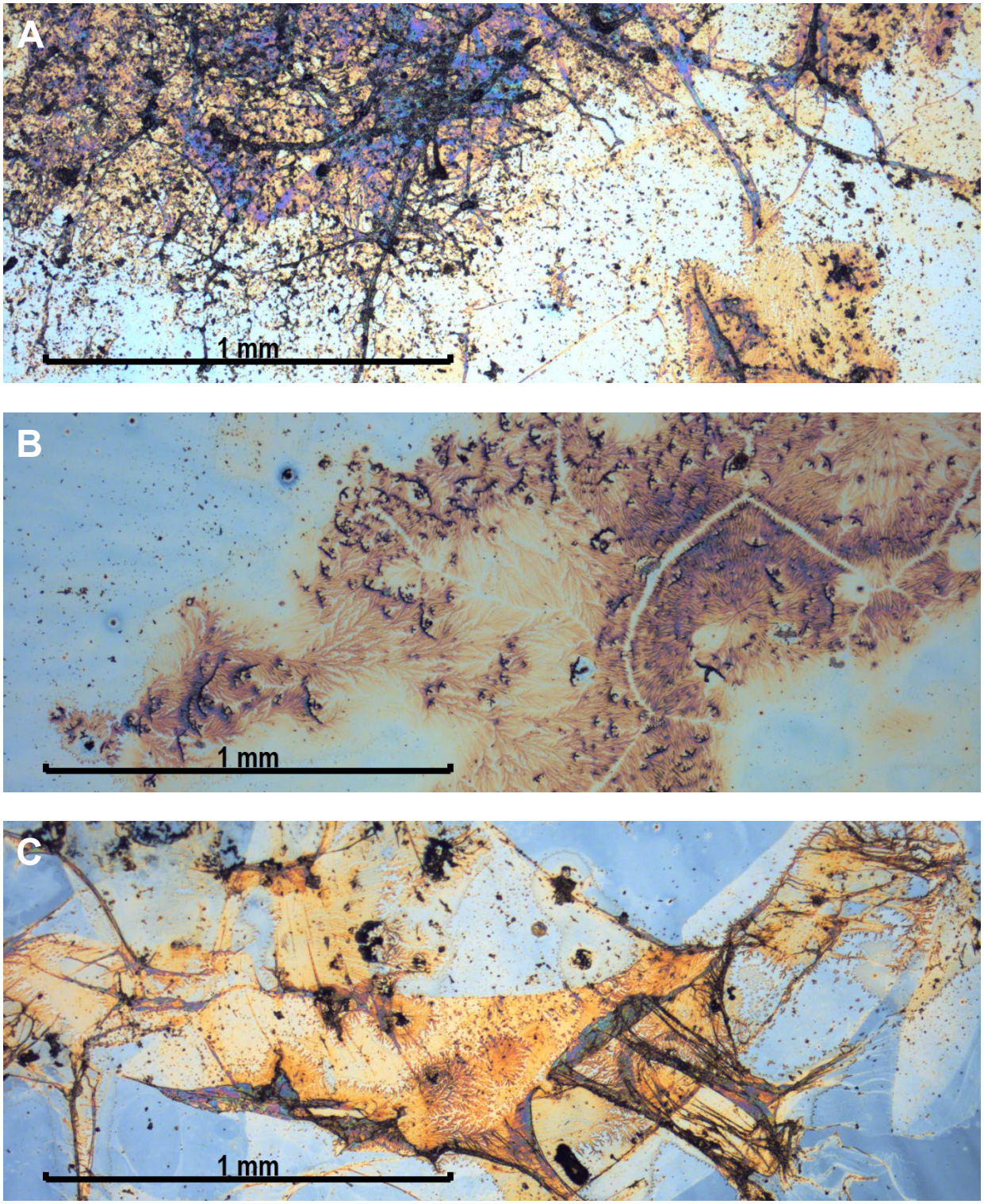

Figure S5. Charged polymer optical imaging at near-macroscopic scale. Cationic surfaces (A) are dominated by amorphous aggregates, anionic (B) by fractal branched structures, and zwitterionic (C) features a mix.

References

1 B. B. Mandelbrot, *The Fractal Geometry of Nature*, W. H. Freeman and Co., 1982.

2 H. E. Stanley, *Fractals Disord. Syst.*, 1996, 1–58.

3 T. G. Smith, G. D. Lange and W. B. Marks, *J. Neurosci. Methods*, 1996, **69**, 123–136.

4 M. W. MOSESSON, *J. Thromb. Haemost.*, 2005, **3**, 1894–1904.

5 R. I. Litvinov and J. W. Weisel, *Matrix Biol.*, 2017, **60**–**61**, 110–123.

6 S. Stamboroski, A. Joshi, P. L. M. Noeske, S. Köppen and D. Brüggemann, *Macromol. Biosci.*, , DOI:10.1002/mabi.202000412.